of Kotel'nikov's theorem; however, a quantitative description of this effect is connected with considerable technical difficulties and fundamental theoretical problems. It should be noted that, unfortunately, this phenomenon is not sufficiently considered in the literature; therefore, let us dwell on it a bit more.

6. Two fundamental questions in computer simulations

First. The final goal of computer simulation is obtaining *information* about the object under study. But then, one should take into account that while it is often possible to pass from one continuous model to another without the loss of information (homeomorphous changes of variables, etc.), *passing from a continuous object to a discrete model, as a rule, leads to information loss*. A simple example is discretization of a reversible linear system on a uniform lattice: as a rule, it is an irreversible mapping. Another example considers the main information characteristic of a dynamical system, its entropy. The entropy is a measure of the exponential increase in the ratio of the number of different trajectories of the system to their length. However, any unambiguous spatial discretization of a system allows only a limited number of infinite trajectories, and the definition of entropy becomes meaningless in this case. Here, we have an evident contradiction between a continuous object and its discrete model; also evident is the necessity to improve the methods of evaluating the entropy of a continuous system from its discretizations. Notice that although different methods of solving this problem have already been proposed, the general task is very difficult to solve. In other cases, the conflict may be less evident but not less dangerous. Hence, the first fundamental question of every computer simulation is: *What is the information loss for the chosen scheme of passing from a continuous object to a discrete one*?

Second. The question is related to the continuous-mathematics analogues of robustness and structural stability. In continuous simulations, if one omits verbal descriptions, this is the question of whether one property or another of the object is tolerant to continuous, smooth, etc. (but necessarily small in some continuous sense) perturbations. However, if we accept that the main point of computer simulations is related to information, we should also pose the following question: *Can we guarantee the information robustness of the chosen scheme of passage from the continuous object to the discrete one*?

Probably, thorough analysis of these questions will be one of the strategic areas of natural sciences in the nearest decades. To give an overall description of the situation in this field is a hopeless task, even more so to predict its development. Some initial progress in this area is reported in Refs [10–12].

This work was supported in part by RFBR (projects Nos 06-01-00256 and 07-07-00031).

References

1. Kotel'nikov V A "O propusknoi sposobnosti 'efira' i provoloki v elektrosvyazi" ("On the transmission capacity of 'ether' and wire in electric communications"), in *Vsesoyuznyi Energeticheskii Komitet. Materialy k I Vsesoyuznomu S'ezdu po Voprosam Tekhnicheskoi Rekonstruktsii Dela Svyazi i Razvitiya Slabotochnoi Promyshlennosti* (The All-Union Energy Committee. Materials for the 1st All-Union Congress on the Technical Reconstruction of Communication Facilities and Progress in the Low-Currents Industry) (Moscow: Upravlenie Svyazi RKKA, 1933) p. 1; second edition: *O Propusknoi Sposobnosti 'Efira' i Provoloki v Elektrosvyazi* (On the Transmission Capacity of 'Ether' and Wire in Electric Communications) (Moscow: Inst. Radiotekhniki i Elektroniki MEI (TU), 2003); *Usp. Fiz. Nauk* **176** 762 (2006) [*Phys. Usp.* **49** 736 (2006)]
2. Kravchenko V F, Rvachev V L *Algebra Logiki, Atomarnye Funktsii i Veivlety v Fizicheskikh Prilozheniyakh* (Algebra of Logics, Atomic Functions and Wavelets in Physical Applications) (Moscow: Fizmatlit, 2006)
3. Whittaker E T "On the functions which are represented by the expansion of interpolating theory" *Proc. R. Edinburgh* (35) 181 (1915)
4. Balakrishnan A V "A note of the sampling principle for continuous signals" *IEEE Trans. Inform. Theory* **3** 143 (1957)
5. Belyaev Yu K "Analiticheskie sluchainye protsessy" ("Analytical random processes") *Teoriya Veroyatnostei Ee Primeneniya* (4) 402 (1959)
6. Beutler F J "Sampling theorems and basis in a Hilbert space" *Inform. Control* (4) 97 (1961)
7. Jerri A J "The Shannon sampling theorem — its various extensions and applications: a tutorial review" *Proc. IEEE* (65) 1565 (1977)
8. Sinitsyn I N *Fil'try Kalmana i Pugacheva* (Kalman and Pugachev Filters) (Moscow: Logos, 1st ed. — 2005, 2nd ed. — 2007)
9. Grigor'ev F N, Kuznetsov N A, Serebrovskii A P *Upravlenie Nablyudeniyami v Avtomaticheskikh Sistemakh* (Control of Observations in Automatic Systems) (Moscow: Nauka, 1986)
10. Kozyakin V S, Kuznetsov N A "Dostovernost' komp'yuternogo modelirovaniya s tochki zreniya teorii informatsii" ("Reliability of computer simulations from the standpoint of information theory") *Informatsionnye Protsessy* **7** 323 (2007); http://www.jip.ru/2007/323-368-2007.pdf
11. Vladimirov I "Quantized linear systems on integer lattices: Frequency-based approach. Part I", CADSEM Report 96-032 (Geelong, Australia: Deakin Univ., 1996)
12. Diamond P, Vladimirov I "Higher-order terms in asymptotic expansion for information loss in quantized random processes" *Circuits, Systems, Signal Process.* **20** 677 (2001)

PACS numbers: **43.30.+m**, **43.58.+z**, 91.50.Ga
DOI: 10.3367/UFNe.0179.200902k.0218

Remote sensing of sea bottom by hydroacoustic systems with complex signals

V I Kaevitser, V M Razmanov

1. Introduction

This report deals with various aspects of applying complex sounding signals with linear frequency modulation (LFM) in hydroacoustic systems (including a multielement antenna) for the exploration of the ocean floor. The report presents a review of theoretical and practical results obtained by authors recently in the course of the development, testing, and implementation under different conditions of the following hydroacoustic systems: acoustic low-frequency linear profilographs, surveillance and interferometric side-looking sonars (SLSs), and multibeam echo sounders.

The radar exploration of planets that was conducted starting in the late 1950s by the group of scientists under the leadership of V A Kotel'nikov resulted in establishing at the Institute of Radioengineering and Electronics (IRE) of the USSR Academy of Sciences (now the Russian Academy of Sciences — RAS) a new field of research — remote mapping of extended objects by high-energy complex sounding signals and digital methods of coherent processing of echo signals. The digital methods of signal synthesizing, recording, and processing, used earlier for planetary radar, in late 1970s were

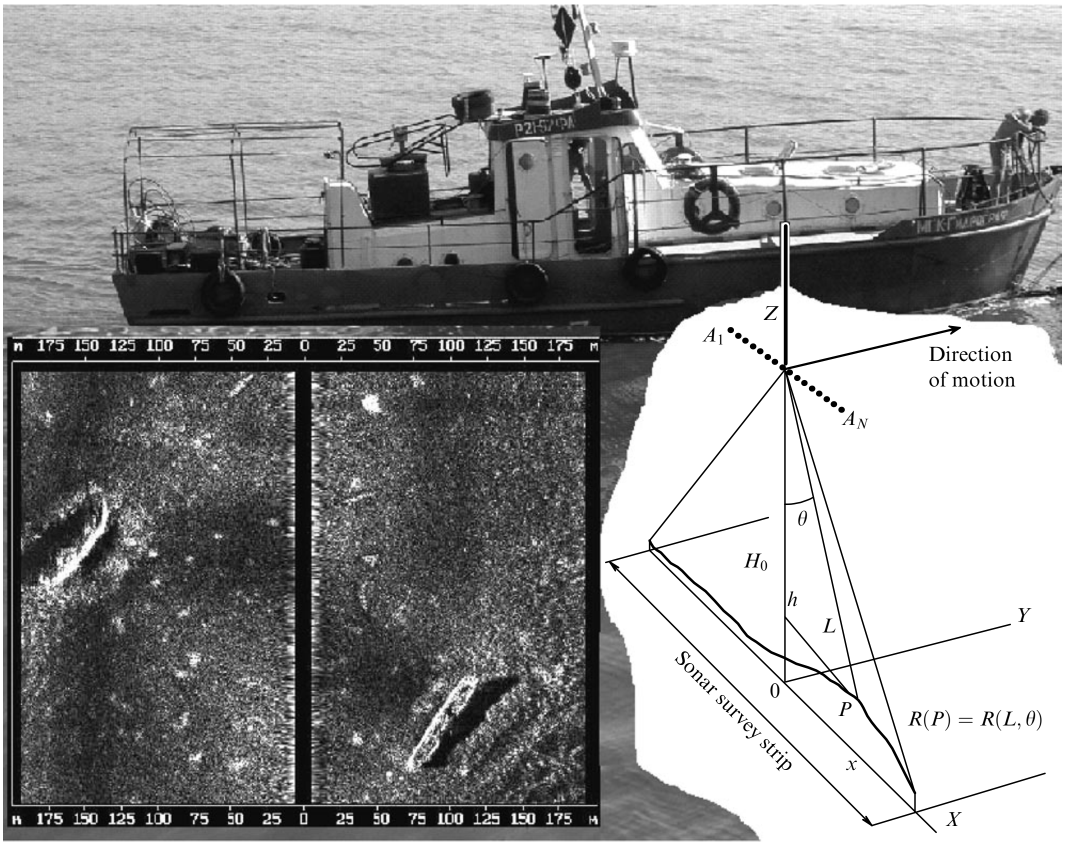

Figure 1. Geometrical sketch of a side-looking sonar survey and a detail of an obtained seafloor acoustic image depicting sunken vessels.

successfully applied to develop a new generation of hydroacoustic systems for seafloor mapping.

Nowadays, the hydroacoustic systems of coherent radar sounding have become the primary tool for remote measurements of the undersea relief and structure of sea bottom deposits. By now, two main classes of systems (somewhat competing with each other) aimed at synchronous measurements of seafloor relief and acquiring bottom surface acoustic images have been developed: interferometric SLSs and multibeam echo sounders [1]. While the surveillance SLS usually contains one onboard antenna and interferometric SLSs two or three antennas, multibeam echo sounders constitute a more complicated system that contains a significantly higher number of receiving elements, usually 100 or more. The studies of subsurface structure of a sea bottom employ low-frequency acoustic profilographs. These are usually one-channel systems that provide continuous profiling of a seabed along a vessel route. The exploration systems are equipped with satellite navigation GPS (Global Positioning System)/DGPS (Differential Global Positioning System), devices for measuring the speed of sound in deep water, and sensors to monitor roll, pitch, and vertical displacements of the vessel. In complex multielement systems, usage of stabilizing equipment reducing vessel rolling effects is justified.

The operational efficiency of coherent sonar systems is determined by the type of sounding signals. For shallow water exploration (up to 100 m in depth), SLS and multibeam echo sounder systems use short sounding pulses with a carrier frequency of up to 500 kHz due to the simplicity of their formation and treatment. For deep water exploration, contemporary systems utilize sounding signals with linear modulation frequency that combine both high-energy capacity and high time resolution.

2. Diagram of side-looking survey

Hydroacoustic methods of side-looking surveys are based on sequential accumulation of seafloor data while the vessel is moving (Fig. 1). The acoustic pulse radiated by the transmitting antenna is sequentially reflected from seafloor elements at different distances. The reflected echo signals are acquired by one or more receiving antennas. The cycle that consists of a pulse transmission and a signal reception forms one realization (one horizontal row of the acoustic image in Fig. 1). A set of sequential realizations that is formed during the vessel movement contains information about scattering characteristics of a seafloor within the sonar survey strip and represents the acoustic image of the floor, similar to optical and radar images. These acoustic images are aimed at visualization and classification of objects. For example, the inset to Fig. 1 shows a detail of the acoustic image of a seafloor area that reveals the fragments of two sunken vessels. The sonar survey strip which is determined by the antenna patterns of receiving elements, power characteristics and the shape of undersea relief is usually set in units of depth H_0, equaling $(4-10)H_0$. The use of antennas with narrow side-looking patterns provides a distinct type of 2-dimensional measurement in a plane of side-looking survey. The seafloor is perceived as a medium with the back scattering factor $R = R(L, \theta)$ dependent on distance L and angle θ between the vertical line and the direction of a signal arriving in a plane of side-looking survey. Considering a coefficient of reflection $R = R(u, \tau)$ as a function of two parameters, namely, the angle parameter $u = \sin\theta$ and time delay τ, the signal $Z_n(t)$ received by a particular antenna in multielement antenna system can be expressed as

$$Z_n(t) = \iint R(u,\tau)\, S_0(t-\tau-\tau_n u)\, \mathrm{d}u\, \mathrm{d}\tau\,, \quad u=\sin\theta\,. \quad (1)$$

Distance L is related to the propagation time (delay) τ as $\tau = 2L/c$, where c is the speed of sound. Additional delay $\tau_n = l_n/c$ caused by geometrical differences in paths at which echo signals reach the various elements of the antenna is determined by coordinate l_n of a particular element in the antenna coordinate system.

In many practical instances that employ complex signals, model (1) can be simplified, limiting itself to a narrow-band approximation. With this in mind, we can present $S_0(t)$ as $S_0(t) = \exp(\mathrm{i}\omega_0 t)\, S_{\mathrm{A}}(t)$, where ω_0 is a carrier frequency, and $S_{\mathrm{A}}(t)$ is a slowly varying component of modulation. Signal $S_0(t)$ will be considered as a narrow-band signal, assuming that under $\Delta t \ll t_0$ the expression $S_{\mathrm{A}}(t+\Delta t) \approx S_{\mathrm{A}}(t)$ is true. As a result, for $\Delta t \ll t_0$ we arrive at the following relationship for a narrow-band signal: $S_0(t_0+\Delta t) \approx \exp(\mathrm{i}\omega_0 \Delta t)\, S_0(t_0)$. Considering arrival time delay $\tau_n u$ on individual elements of the array as small parameter Δt of theory, in other words, given that $\tau_n u \ll t-\tau$ is true, measurement model (1) can be presented as follows:

$$\begin{aligned} Z_n(t) &= \iint R(u,\tau)\, S_0(t-\tau) \exp(-\mathrm{i}\omega_0 \tau_n u)\, \mathrm{d}u\, \mathrm{d}\tau \\ &= \int R_t(u) \exp\left(-2\pi\mathrm{i}\,\frac{l_n}{\lambda}\,u\right) \mathrm{d}u\,, \end{aligned} \quad (2)$$

where $R_t(u) = \int R(u,\tau)\, S_0(t-\tau)\, \mathrm{d}\tau$, and λ is a wavelength that is related to the carrier frequency ω_0. For fixed distances, the determination of the reflection coefficient is a task of spectral estimation, i.e., assessment of the acoustical spectrum of a signal based on a set of its discrete samples Z_n:

$$Z_n = \int R_t(u) \exp\left(-2\pi\mathrm{i}\,\frac{l_n}{\lambda}\,u\right) \mathrm{d}u\,. \quad (2a)$$

Here, $R_t(u)$ can be considered the angular spectrum that may be estimated by the well-known spectral analysis methods of both a parametric and nonparametric nature [2, 3]. The task of data processing is the estimation of reflection coefficient $R(u,\tau)$ based on a set of measurements of $Z_n(t)$ and subsequent determination of parameters of a seafloor. The applied methods of estimation of the reflection coefficient R and parameters of a seafloor, as well as various limitations related to variations in the shape of an undersea relief, differ from each other depending on the number of receiving antennas in the measuring systems employed.

3. One-channel systems with linear-frequency-modulated signals: acoustic profilographs and surveillance side-looking sonars

In one-channel systems, in the absence of angular selectivity, measurement model (1) degenerates into the relationship for the coefficient $R = R(\tau)$ which is dependent on delay τ (distance L) only; thus, the registered signal is described as

$$Z(t) = \int R(\tau)\, S_0(t-\tau)\, \mathrm{d}\tau\,.$$

In a mean-square metric, the $R(\tau)$ estimate should minimize the functional

$$\begin{aligned} \varDelta = \int \mathrm{d}t \left(Z - \int S_0(\tau)\, R(t-\tau)\, \mathrm{d}\tau\right) \\ \times \left(Z^* - \int S_0^*(\tau)\, R^*(t-\tau)\, \mathrm{d}\tau\right). \end{aligned} \quad (3)$$

The optimum estimate of $R(t)$ must satisfy the Fredholm integral first-order equation

$$\int Z(t+\tau)\, S_0^*(\tau)\, \mathrm{d}\tau = \int R(t-\tau)\, K_0(\tau)\, \mathrm{d}\tau\,, \quad (4)$$

where the kernel is determined by the correlation function of a sounding signal:

$$K_0(\tau) = \int S_0(t)\, S_0^*(t+\tau)\, \mathrm{d}t\,.$$

For LFM signal $S_0(t) = \exp\left(\mathrm{i}\omega_0 t + \mathrm{i}(\Delta\omega/2T)t^2\right)$, the correlation function looks like

$$K_0(\tau) = \exp\left(\mathrm{i}\Phi(\tau)\right) \frac{\sin\left[\pi B(\tau/T_0)\left(1-|\tau|/T_0\right)\right]}{\pi B\tau/T_0}\,, \quad (5)$$

where $\Phi(\tau) = -(\omega_0 + \pi B/T)\tau$, B is a base of a signal, defined as $T_0\Delta\omega = 2\pi B$, T_0 is a pulse length, and $\Delta\omega$ is a bandwidth.

Strictly speaking, equation (4) falls into a class of ill-posed problems. A number of methods that allow solving these problems use various additional assumptions about the changing character of $R(\tau)$ [4]. In practice, relationship (4) is employed as a ready-made algorithm of approximate estimation of $\tilde{R}(\tau)$ for a given resolution. To demonstrate it we present expression (4) as two relationships:

$$\tilde{R}(t) = \int Z(t+\tau)\, S_0^*(\tau)\, \mathrm{d}\tau\,, \quad (6a)$$

$$\tilde{R}(t) = \int R(t-\tau)\, K_0(\tau)\, \mathrm{d}\tau\,. \quad (6b)$$

Relationship (6a) can be regarded as a treatment algorithm that is realized in a spectral range with the help of fast Fourier transform (FFT) algorithms. The operation of a signal compression is the price for employing complex signals. Relationship (6b) defines resolution of the $\tilde{R}(\tau)$ estimate as a convolution of the exact solution with the kernel $K_0(\tau)$ — the correlation function of a sounding signal. For tone signals, the correlation interval (area where the value of $|K_0(\tau)|$ differs from zero significantly) is determined by the pulse duration T_0. The main advantage of employing LFM-probing signals is that due to intrapulse modulation the correlation interval decreases to T_i/B, where B is a signal base. This allows us to combine high energy potential with high (up to fractions of the centimeter) resolution.

The dependence of the modulus of reflection coefficient R on the distance serves as the basis for acoustic seafloor mapping. The absence of angular selectivity in one-channel surveillance SLSs does not prevent employing this class of systems for exploration of relatively flat seafloor areas in searching for small-sized objects and details of undersea relief such as furrows, trenches, and stones. Usually, the surveillance SLS constitutes a one-channel acoustic sonar mounted on the right and left sides of the shipboard and is equipped

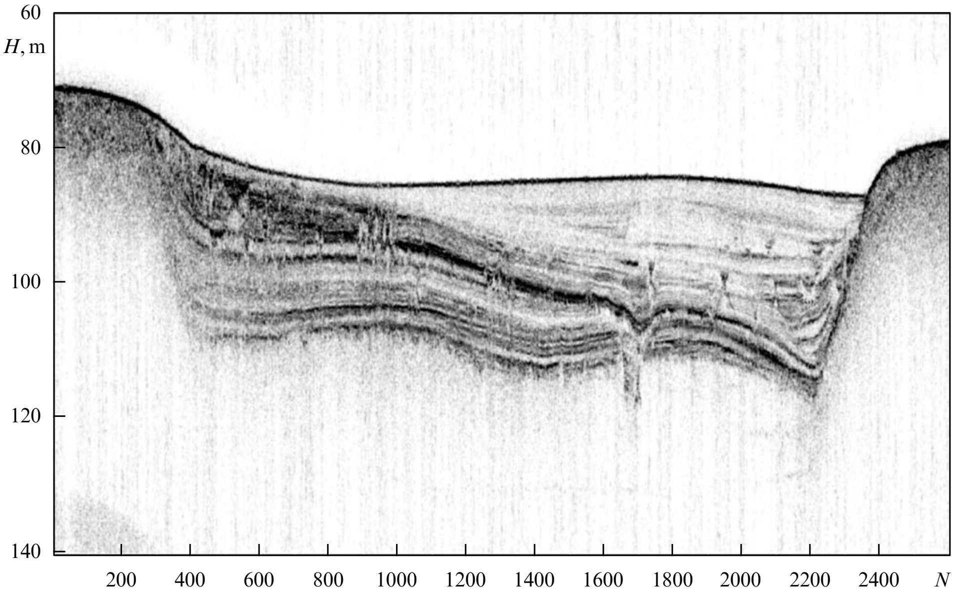

Figure 2. Profile of undersea relief and sedimentary rocks (Chukchi Sea). Probable ancient riverbed.

with independent transceiver antennas having a narrow (around 1°) directional pattern along the route of a vessel, as well as a digital system for generating, recording, and treating signals. The type of radiated pulse comprises both tonal and LFM sendings. Operating frequencies fall within 10–500 kHz. In tonal mode, the pulse duration is several fractions of a millisecond, while in LFM mode it reaches several seconds.

Among one-channel devices that broadly employ LFM signals in experimental samples are acoustic linear profilographs. Many years of experience using low-frequency profilographs with LFM-probing signals (the ones that have been developed at IRE RAS) has confirmed their good operational abilities and helped to reveal some specifics in interpreting obtained results. The profilograph operating frequency equals 5 kHz, band frequency is around 4 kHz, and radiated power is near 3 kW. The profilograph comprises a 9-element antenna system, electronic system for generating probing sonar signals (digital synthesizer), sound projector, and computer data input interface. The device contains a digital system for collecting, mapping, and processing data. It is intended for use in exploration of a seafloor topography and structure of sea bottom deposits in a range of depths from 20 to 3000 m. Data collection programs provide coherent engagement of echo signals, input of navigational information about vessel location from GPS sensors, real-time data imaging, and archiving of the processed data.

Figure 2 shows a detail of an undersea relief that was acquired in the course of seabed profiling in the deep freezing waters of the Chukchi Sea at a depth of approximately 70 m. The result of profiling shows high interference immunity of the device, providing a high-resolution image of seabed deposits. The above detail attracts more interest because it clearly depicts a depression filled with deposits. This image resembles a riverbed of an ancient river after the land submerged as a result of a rise in the sea level. The offered hypothesis may serve as a very productive approach to solving some problems in the course of establishing continental shelf boarders.

The high energy potential of LFM-probing signals allows conducting the profiling of seabed deposits at quite large depths. Figure 3 presents the results of profiling in the Sea of Japan at depths of 1200–1400 m. The studied area is characterized by varying relief with a thick stratum of layered deposits. The first reflection corresponds to the depth and it is confirmed by the measurements made with single- and multibeam echo sounders. The horizontal axis is the distance travelled in meters; the vertical axis is the depth in meters. As indicated in Fig. 3, the depth of profiling is more than 100 m; slope deposits have the layered structure which is typical of silted clay. In the area of the depression, the character of the profilogram is more homogeneous over the depth, typical of sandy clay soils.

4. Signals with linear frequency modulation in interferometric side-looking sonars

The complex interferometric SLS system that is used for the analysis of an undersea relief within the sonar survey strip includes additional receiving channels that contain a set of antennas in a vertical plane. In interferometric SLSs, signal processing is based on the assumption that at any given distance the present signal propagates in a single direction: $R(u,\tau) = R(\tau)\,\delta\big[u - u_0(\tau)\big]$, therefore, reception model (2) in a narrow-strip approximation becomes

$$Z_n(t) = R(t)\exp\left[2\pi\mathrm{i}\,\frac{l_n}{\lambda}\,u_0(\tau)\right],$$

where $R(t) = \int R(\tau)\,S_0(t-\tau)\,\mathrm{d}\tau$, and $u_0 = \sin\theta_0$. The determination of reflection coefficient $R(t)$ is exactly the same as in a surveillance SLS. To calculate the angle of signal arrival we need to measure the phase Ψ of a complex-conjugate product of the pair of samples in two channels (interferometer):

$$A_{n,m}(t) = Z_n(t)Z_m^*(t) = \big|R(t)\big|^2\exp\Psi_{n,m}\,,$$
$$\Psi_{n,m} = \arctan\frac{\operatorname{Im}A_{n,m}}{\operatorname{Re}A_{n,m}}\,. \qquad (7)$$

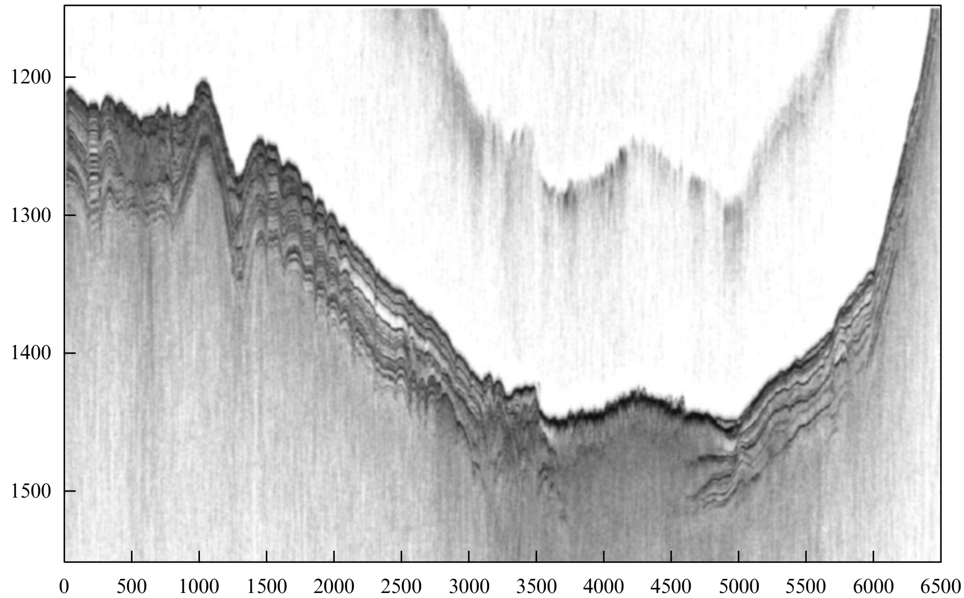

Figure 3. Detail of profiling a sea bottom deposit in the Sea of Japan at depths of up to 1500 m. The depth of profiling the subsurface bottom structures is more than 100 m.

The interference phase is related to both the angle of arrival θ and the interferometer base $b_{nm} = l_n - l_m$ as follows:

$$\Psi_{n,m}(t) = \exp\left[2\pi i \frac{b_{nm}}{\lambda} \sin\theta(t)\right].$$

The phase is used to calculate the angle of arrival, while the depth h and horizontal coordinate x of the reflection element (relief) are calculated from the distance L and angle of arrival θ using the relationships

$$h = L\cos\theta, \qquad x = L\sin\theta. \tag{8}$$

The details of processing the data obtained by interferometric SLSs are described in Refs [6, 7].

Commonly used interferometric SLSs contain 2–3 antennas on each side of a shipboard (several interferometers), a satellite navigation system, devices for profiling the speed of sound, and sensors to monitor the roll, pitch, and vertical displacements of a vessel. Similar to one-channel systems, interferometric SLSs have a directional pattern that is narrow (near 1°) along the line of motion and rather wide (near 60°) in the plane of the side-looking sonar survey. This type of acoustic system is broadly used since it is easy to operate and has a wide survey strip of observation. These systems produce high-quality acoustic images and at the same time allow measuring the depths within the survey strip.

Various modifications of experimental interferometric SLSs developed at IRE RAS have been successfully employed in different applications from river floor soundings to a large-scale exploratory projects carried out on large-capacity ships in the deep freezing waters of the Arctic Ocean [5–7]. Surveying work in shallow waters (up to 100 m) mostly employs tone acoustic pulses that do not require any compression. On the other hand, work in deep waters employs LFM signals of various duration depending on depth and the desired energy characteristics.

We have to note the important differences in applying tone and LFM signals. In acoustic images created by tone signals, the prime elements on both the left and right sides contain a characteristic flare. This is caused by amplitude overload of the detectors. In practice, it significantly complicates the circuitry of the receiving device because it requires engaging a temporal automatic gain control (TAGC) for each reception row. This imposes considerable difficulties in data processing and requires manual operator intervention. The quality of produced images greatly depends on acoustic noises of various natures. In coherent processing of complex signals, the extraction of useful information is done along the frequency rather than amplitude characteristics. This problem is nonexistent when coherence of echo signals is retained. In such cases, the use of a conventional system of AGC is a sufficient means for matching a level of output signal with the dynamic range of the analog-to-digital converter (ADC). The latter provides an important advantage to the above remote sounding systems in uncrewed submersible vehicles and in cases of significant amplitude interferences.

Figure 4 depicts details of acoustic images obtained in the course of studying the route of an undersea optical cable in the icy conditions of the Arctic Ocean. Figure 4a shows traces of sea bottom exaration caused by a large iceberg, and Fig. 4b demonstrates trenches of the same nature. The complex trajectory of the trenches is related to the changing direction of underwater currents. Besides images of the objects themselves, the acoustic images contain information about the acoustic density of a sea bottom surface. The difference in back scattering factors is determined by the degree of background brightness. It carries information about the geological bedrock on the sea bottom. Figure 5 presents a detail of a bathymetric chart built on the results of interferometric measurements. Halftone images exhibit the fluctuations in seabed density.

The main deficiency of interferometric systems is the distortions in the selectivity of signals detected with the same delay with respect to the angle of arrival. This results in limitations on using these systems in multibeam applications, as well as in cases of a complex undersea relief, etc. [6]. Multielement systems are free of such limitations; they allow separating signals coming from different directions (para-

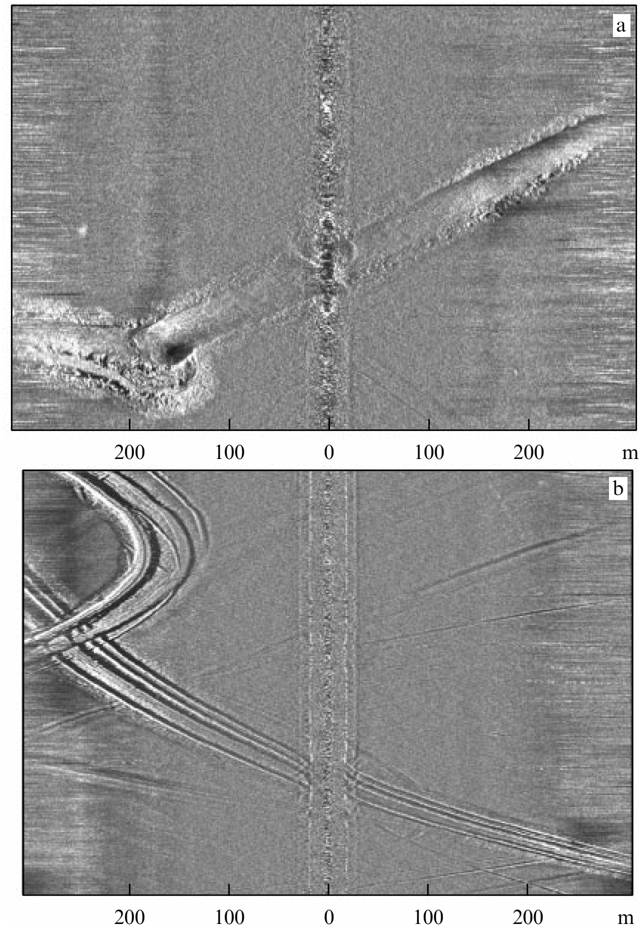

Figure 4. Details of acoustic images provided by an interferometric SLS with an LFM-probing signal: (a) bottom tracks are traces of exaration caused by a large iceberg in the Arctic Sea at a depth of 20 – 30 m; the vertical length of the detail is 1 km; (b) ice exaration that characterizes the trajectory of iceberg movement in changing currents; vertical length of the detail is around 2 km.

metric approach) or signals with high angular resolution (nonparametric methods).

5. Miltibeam echo sounder with linear-frequency-modulated sounding signals

In a multielement array and in measurement model (1), the mean-square criterion (3) for estimation of the reflection coefficient takes the form

$$\varDelta = \sum_n \int \left| Z_n(t) - \int R(u,\tau)\, S_0(t-\tau-\tau_n u)\, \mathrm{d}u\, \mathrm{d}\tau \right|^2 \mathrm{d}t\,,$$

while the equation for the estimate is written out as

$$\sum_n \int Z_n(t)\, S_0^*(t-\tau_0-\tau_n u_0)\, \mathrm{d}t = \int R(u,\tau) \left\{ \sum_n K_0\big(\tau-\tau_0-\tau_n(u-u_0)\big) \right\} \mathrm{d}u\, \mathrm{d}\tau\,.$$

The kernel (enclosed in curly brackets) of the integral equation describes the resolution in angle and distance. In the narrow-band approximation, the kernel degenerates into a product of two factors dependent on angle and distance:

$$\sum_n \tilde{Z}_n(t) \exp\left(2\pi \mathrm{i}\, \frac{l_n}{\lambda}\, u_0\right) = \int R(u,\tau)\, K_0(\tau-t)\, K_\theta(u-u_0)\, \mathrm{d}u\, \mathrm{d}\tau\,, \qquad (9)$$

where $\tilde{Z}_n(t) = \int Z_n(t)\, S_0^*(t-\tau_0)\, \mathrm{d}t$ is the compressed input data, and $K_\theta(u-u_0) = \sum_n \exp\big(-2\pi \mathrm{i}(l_n/\lambda)(u-u_0)\big)$ is a directional pattern of the array. Similar to the equation from Section 3, equation (9) can be considered an estimate of the reflection coefficient $\tilde{R}(u,\tau)$ within the framework of time resolution of the correlation function $K_0(\tau)$ and angular resolution of directional pattern $K_\theta(u)$:

$$\tilde{R}(u,t) = \sum_n \tilde{Z}_n(t) \exp\left(2\pi \mathrm{i}\, \frac{l_n}{\lambda}\, u_0\right). \qquad (10)$$

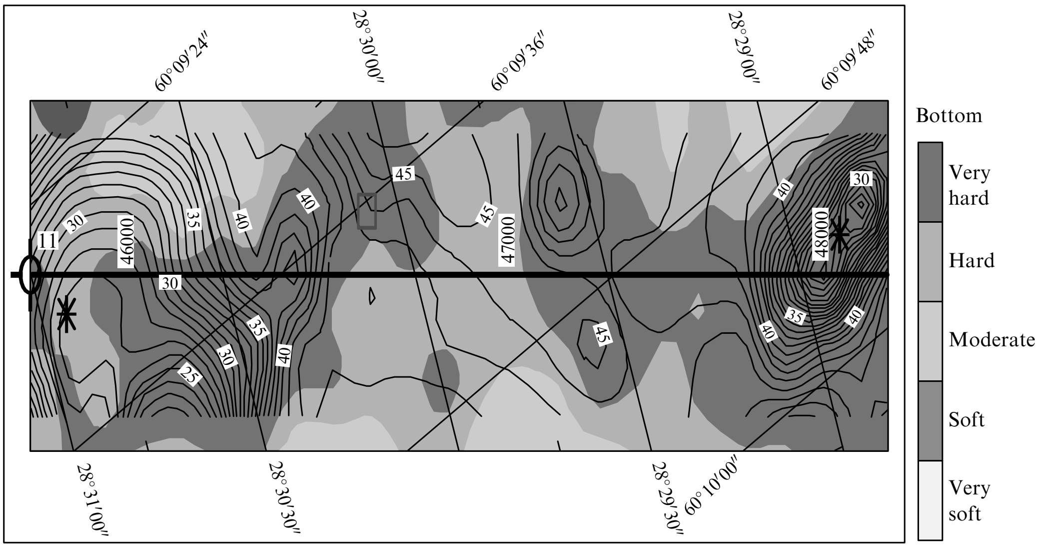

Scale 1:10000, Ellipsoid WGS84, Projection UTM, Center Meridian27°

Figure 5. Portion of a bathymetric chart in the form of contour lines of depths (isobaths). The isobaths shown have a 5-m pitch. The halftone background marks the acoustic density of the bottom.

In this case, signal processing constitutes a compression of input samples in all channels and Fourier transformation of these samples for each distance. For a fixed pattern, especially with a small number of receiving antennas, an increase in spatial resolution becomes an important practical goal. The solution to this problem can be found with the help of both equation (9) (nonparametrical approach) and the use of parametrical algorithms of spectral estimation [2–4].

The first tests of an experimental system with a multi-element antenna and LFM-probing signals were conducted at IRE RAS in 2007 at an aquatorium on the Sea of Japan. This hydroacoustic system consists of a linear transmitting and 32-element receiving antenna system (modelled on the Mills cross), powerful amplifier of radiated signals, digital generator (synthesizer) of LFM signals, and 32-channel low-noise digital receiver with computer input data interface. The carrier frequency of sounding signals is 30 kHz, frequency deviation is 3.0 kHz. Signal quantization was carried out at a frequency of $\sim$ 6.0 kHz in each of the channels. The distance between receiving elements of the antenna array is a half wavelength of the radiated signal at the carrier frequency.

In accordance with formula (10), compression in all 32 channels of signals was carried out initially. The calculation of the angular spectrum for each distance was performed with the help of FFT with $N = 32$ dimensions (in some cases a larger dimension, up to $N = 256$, was used) and by weighting the input channel samples for different variants of weighted sequences. In this case, the set of spectral samples forms a system of partial beams. The angular position $u_m = \sin\theta_m$ of a beam with number (spectral sample) m for distance d between receiving elements of an antenna with a half wavelength λ is derived from relationship $u_m = \lambda m/(dN) = 2m/N$, where $m = 0, \ldots, N-1$, N is the FFT dimension, and the angle θ is measured from the antenna normal. Beam amplitude reaches its maximum at a distance corresponding to the point where the beam crosses the sea bottom. The generation of the undersea relief was performed using slant range L, which had been determined by the position of the amplitude maximum peak in each beam with a known angle of inclination in accordance with expressions (8). Examples of variation of beam amplitude near the maximum are shown in Fig. 6 and characterize two extreme types of data. For the first group of data (in the left part of Fig. 6a), the peak near the maximum is wide, and its amplitude smoothly decreases along the ascending beam number (angle of inclination), shifting in distance. The FFT algorithm applied to the spatial diagram forms a good image of a seafloor relief (an example of this type of relief is shown in Fig. 6b). For a second group of data (in the right part of Fig. 6a), the shape of the amplitude near the maximum looks like a narrow peak along almost the same distance; the peak amplitude declines sharply with ascending beam number. The treatment of data revealed that the use of FFT in such cases is inefficient due to a high level of side lobes; therefore, estimation of the angular spectrum was performed on the basis of the autoregressive parametric method (Proni method) [2]. This demonstrates good timing for the development and application of spectral methods of estimation with high resolution in multibeam systems.

6. Conclusion

The presented results of theoretical analysis and developed algorithms of signal processing in various hydroacoustic systems with LFM-probing signals for remote seafloor exploration have been implemented and tested under different conditions, including complicated operation in Arctic waters.

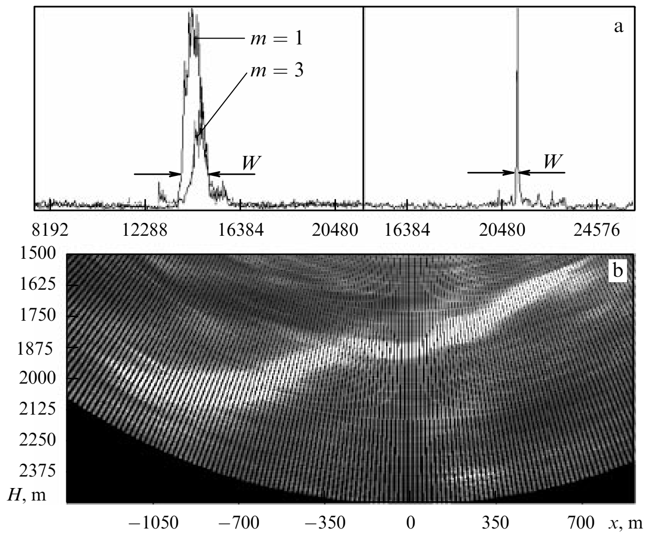

Figure 6. Variation of echo signal amplitude of individual beams versus distance (sample number); m is the beam number. The sampling period corresponds to a distance interval of 0.1 m. (Obtained in the course of probing various types of bottom soils.) (b) Example of relief extraction from the system of spatial beams.

This report outlines only some aspects of treating data in LFM-signal applications. Certain important issues, such as methods of secondary data treatment, the construction of bathymetrical maps and maps of brightness, preparation of various reports, and documenting the results, are beyond the scope of this presentation.

The conducted experiments have proved the important advantages of such development projects in comparison with traditional hydroacoustic sonars that employ tone sounding pulses. These advantages include an increase in energy potential and resolution; higher interference immunity that results in improved electrical and acoustical compatibility of various devices, and increased potential for automation of various hydroacoustic systems.

Besides the above aspects, the application of coherent methods of LFM-signal processing in promising projects will in the future allow employing additional signal characteristics that may become important classification criteria for interpreting the results of remote sea bottom studies [8].

References

1. Costnel C, Yoos L T *Sea Technol.* (March) (2007)
2. Marple S L *Digital Spectral Analysis: with Applications* (Englewood Cliffs, NJ: Prentice-Hall, 1987) [Translated into Russian (Moscow: Mir, 1990)]
3. Leonowicz Z, Lobos T, Rezmer J *IEEE Trans. Industrial Electron.* **50** 514 (2003)
4. Vasilenko G I *Teoriya Vosstanovleniya Signalov* (Theory of Signal Reconstruction) (Moscow: Sov. Radio, 1979)
5. Kaevitser V I et al. *Radiotekhnika* (1) 42 (2004)
6. Kaevitser V I, Razmanov V M *Radiotekhnika* (12) (2005)
7. Razmanov V M, Krivtsov A P, Dolotov S A *Radiotekh. Elektron.* **51** 58 (2006) [*J. Commun. Technol. Electron.* **51** 52 (2006)]
8. Gulyaev Yu V, Zakharov A I, Kaevitser V I *Dokl. Ross. Akad. Nauk* **413** 257 (2007) [*Dokl. Earth Sci.* **413** 327 (2007)]